In situ focus characterization by ablation technique to enable optics alignment at an XUV FEL source

N. Gerasimova,[1,a),b)] S. Dziarzhytski,[1] H. Weigelt,[1] J. Chalupský,[2] V. Hájková,[2] L. Vyšín,[2] and L. Juha[2]

[1]*Deutsches Electronen-Synchrotron DESY, Notkestrasse 85, 22607 Hamburg, Germany*
[2]*Institute of Physics, Academy of Sciences of the Czech Republic, Na Slovance 2, 18221 Prague, Czech Republic*

(Received 4 March 2013; accepted 14 May 2013; published online 3 June 2013)

In situ focus characterization is demonstrated by working at an extreme ultraviolet (XUV) free-electron laser source using ablation technique. Design of the instrument reported here allows reaching a few micrometres resolution along with keeping the ultrahigh vacuum conditions and ensures high-contrast visibility of ablative imprints on optically transparent samples, e.g., PMMA. This enables on-line monitoring of the beam profile changes and thus makes possible *in situ* alignment of the XUV focusing optics. A good agreement between focal characterizations retrieved from *in situ* inspection of ablative imprints contours and from well-established accurate *ex situ* analysis with Nomarski microscope has been observed for a typical micro-focus experiment. © *2013 AIP Publishing LLC*. [http://dx.doi.org/10.1063/1.4807896]

I. INTRODUCTION

The novel type of extreme ultraviolet (XUV) and X-ray sources, the free electron lasers (FELs) such as FLASH in Germany,[1] LCLS in USA,[2] or SACLA in Japan[3] produce unprecedentedly intense short pulses of coherent short-wavelength radiation and enable a large variety of novel experiments being performed for the first time. The radiation from these sources resembles partially that from classical lasers and partially that from synchrotrons, so that to handle this radiation, new dedicated methods and instrumentation merging expertise from different fields should be developed. For instance, though the beam transport systems are very similar to the beamlines at the synchrotron sources, the diagnostics methods are often adopted from the laser optics. In particular this is valid for the focus characterization. The knife edge scanning method, which is standard at synchrotron beamlines, is successfully used at FEL sources.[4] Yet, scanning is limited to average properties diagnostics while most of presently operational XUV and X-ray FELs[1–3] often demonstrate stochastic behavior: when the lasing is based on self-amplified spontaneous emission (SASE) process, each pulse is particular and single pulse diagnostics is needed to enable a comprehensive insight. The imaging of XUV and X-rays into visible fluorescence by imaging crystals can provide a single pulse diagnostics. Imaging crystals are often used, especially, to monitor relatively large spots. However, the method is limited by saturation and quenching of the fluorescence process and demands for strong attenuation of intense FEL beam. This necessity to keep the fluorescence level below saturation restricts single pulse detection of strongly focused beams: when the spot size is reduced to sub-10 μm, high-magnification inspection system is required; increase of magnification, in turn (as the working distance and numerical aperture are fixed) put stronger requirements on camera sensitivity. This limitation on detectable spot size, set by low number of fluorescence photons, becomes most pronounced in XUV regime for the small penetration depth of XUV photons (compared to X-rays) limits the number of visible photons to be detected even more.

There are two other methods, both adopted from laser optics, which are used to characterize highly focused beam at the short wavelength FELs: the wavefront reconstruction using, for instance, Hartmann plate[5,6] and the beam profiling by ablative imprints.[7,8] The wavefront reconstruction is a powerful and sensitive method since it can provide both phase and amplitude information. However, the measurements are done behind the beam waist in this case, and the reconstructed beam profile in focus depends strongly on degree of spatial coherence; the latter cannot be simply predicted and should be measured for such a source as FLASH.[9] On the other hand, detailed knowledge on wavefront is not required for the focusing optics alignment and focal spot size estimation. In return, the ablative imprints, which are taken in the beam waist position and enable direct visualization of the beam profile in focus, can provide convenient diagnostics for XUV optics alignment. Yet, a combination of two technical challenges hindered the method being easily applied to *in situ* focusing optics alignment at the XUV/soft X-ray FEL beamlines. First, this is a demand for ultrahigh vacuum conditions necessary to operate the XUV/soft X-ray optics. Second, *in situ* microscopy inspection is challenged by optical transparency of the samples to be ablated, e.g., PMMA (poly(methyl methacrylate)) which has been shown to be an ideal substance for the imprints in case of XUV radiation.[7] Here we report on a solution found to overcome the challenges mentioned above and present a compact and low-cost tool enabling *in situ* focus diagnostics and XUV optics alignment using ablation imprints technique.

[a)]Author to whom correspondence should be addressed. Electronic mail: natalia.gerasimova@xfel.eu
[b)]Present address: European XFEL GmbH, Albert-Einstein-Ring 19, 22761 Hamburg, Germany.

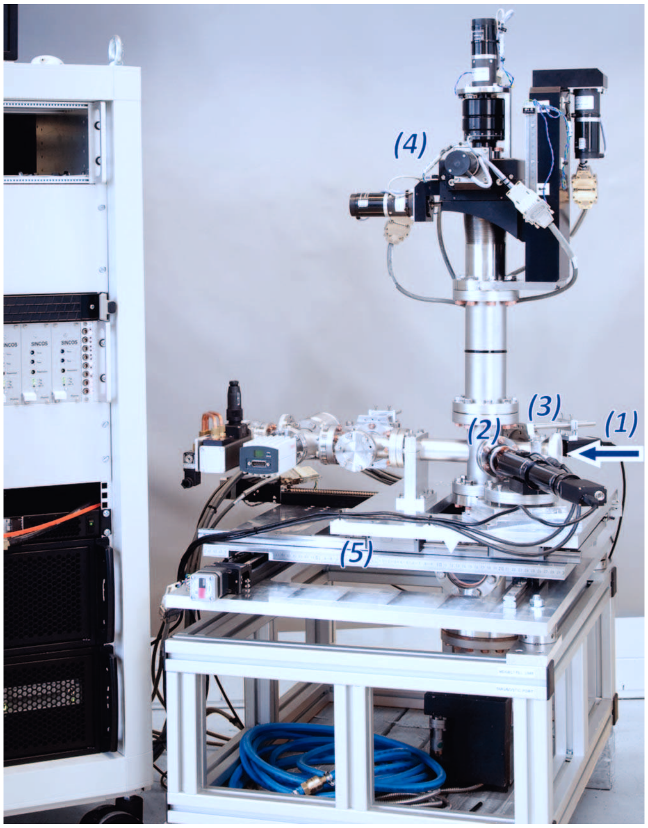

FIG. 1. The diagnostics port for *in situ* focus characterization: (1) the FEL beam comes from the right; (2) the optical port for ablative imprints inspection equipped with the microscope optics and the CCD is directed towards the viewer at 60° to the FEL incoming beam; (3) the port for imaging crystal inspection is directed from the viewer at 45° to the FEL beam; (4) the sample positioning is enabled by a rotatable feedthrough combined with an X-Y stage from top; (5) the X-Y stage from below allows for caustic scans.

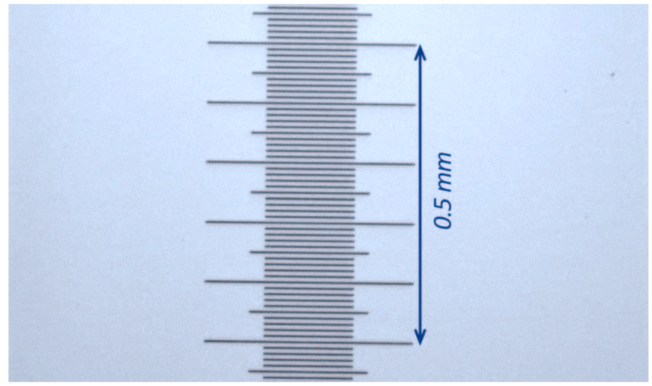

FIG. 2. Taken *in situ* image of 10 μm per division scale.

II. THE INSTRUMENT

A dedicated diagnostics port for focus characterization has been designed and built up to enable *in situ* alignment of XUV focusing optics at FLASH (Fig. 1). The goal was set to approach 3 μm resolution in spot inspection which would enable aligning of the beamline optics aiming down to 5 μm focus size. To reach such a resolution maintaining at the same time ultrahigh vacuum conditions, a solution of commercial optical microscopy system operated in air (outside the vacuum chamber) has been chosen to image an imprinted spot on a sample onto a CCD. The resolution in such scheme is limited by a minimum distance needed to separate the optical system from the sample in vacuum. In our case the working distance of above 78 mm is given by an optical window mounted at 60° with respect to the incoming FEL beam. This geometry allows for direct inspection of ablative imprints while the sample, faced towards the microscope (inspection system), is being shot with single FEL pulses. The sample positioning is enabled by a rotational feedthrough combined with X-Y translation stage (Fig. 1). There is a possibility foreseen to face the sample in any other direction, e.g., towards the FEL beam, for shooting and rotating towards the microscope for inspection just afterwards.

The optical microscopy system has been realized with a Navitar high magnification zoom lens 12×-zoom approaching 1.65 μm resolution at the closest possible working distance of 78 mm. The Basler scA1600 CCD has been chosen as a detector resulting in 0.66 μm per pixel calibration factor for high magnification mode. The calibration measurements presented in Fig. 2 show high quality of the imaging which is an important advantage of commercially developed standard microscope lenses. In addition, the commercial in air solution is provided with a good optical tightening, which is a challenge for in-vacuum conditions (for instance, commonly used in air anodized materials are incompatible with ultrahigh vacuum). And finally, commercial solutions allow for a proper illumination system, which is a key to overcome the problem of low contrast when structures on optically transparent samples are to be inspected. To achieve high contrast in ablative imprints inspection, an intense coaxial illumination, BrightLight LED from Navitar, has been chosen. An idea of coaxial illumination is important since it allows the light being reflected back from the smooth surface with an exception of the structures having slope to the surface. In return, the core of the ablative imprints method is the detection of imprints contours corresponding to the damage threshold and thus tracing the beam profile along with changeable intensity of the beam.[7,8,10] And, for the contours are always under a certain slope to the surface, the coaxial illumination allows to monitor them with high contrast. The sample angular position is easily adjustable with the rotational feedthrough aiming for strongest back-reflection. Finally, we do not discriminate any negative influence of the optical window (the latter was provided with antireflection coating) separating the inspection system from in-vacuum environment.

The organic molecular solids such as PMMA have been shown to be a proper substance to characterize focused XUV beam by ablative imprints technique.[7] We prefer to use the PMMA thin layers deposited onto monocrystalline Si substrates by spin coating process (fabricated by Silson Ltd., UK). The layer thickness varying from 500 nm to 5 μm provides adjustment for the flux level. The imprints on spin-coated PMMA samples have been compared with those on bulk PMMA samples provided by Goodfellow and higher sensitivity has been achieved in the first case. We attribute this observation to higher surface quality of the deposited PMMA layers compared to polished bulk. The highest surface quality in this case is important for ablation itself and in addition ensures high contrast of inspection discussed above.

A translation stage below (Fig. 1) allows both adjusting the set-up transversally to the beam and scanning along the beam waist to enable caustic measurements and beam characterization along the beam propagation axis.

Finally, the diagnostics port is compact and allows for fast exchange of samples or installation to the beamline due to small volume and easy pumping down to the operational conditions of 10^{-9} mbar range (ensuring safe operation of beamline focusing mirrors).

The ablative technique can be complemented both with the wavefront measurements, for a possibility to install the Hartmann wavefront sensor behind the tool is foreseen, and with the imaging of the XUV radiation into visible fluorescence. The latter is enabled by the imaging crystal; we use 0.1 mm thick YAG doped with 0.2% Ce from Crytur Ltd., Czech Republic, mounted onto the same sample holder as the samples for ablation. Conceptually, the fluorescence spots which image FLASH radiation could be seen by the same microscope system as for the ablation technique in absence of illumination. In practice, however, this high magnification inspection does not work in single shot regime due to above-mentioned requirements put by low fluorescence level on camera sensitivity. The limited fluorescence level results from a demand to stay below saturation along with small volume emanating these photons. The latter is related to extremely small penetration depth of XUV photons: at FLASH operating below C K-edge, the penetration depth is below 100 nm in case of YAG:Ce crystals. This limitation on number of fluorescence photons becomes stronger for lower XUV photon energies and smaller spots and does not allow for high magnification with a simple CCD detector in our case. More sensitive cameras, e.g., intensified CCD, are not only much more expensive but bulky as well. To increase the photon flux on a CCD, an additional optical system of moderate resolution has been added. This system consists of Pentax C5028 lens and Basler scA1300 CCD and mounted on the second window port at 45° to the incoming FEL beam (Fig. 1). The crystal can be faced towards this port by the rotational feedthrough. The scaling factor of the optical system is 5.9 μm per pixel, and a resolution of 12 μm is reachable. This imaging technique can be used for spot characterization down to 20 μm in size.

III. ABLATIVE IMPRINTS AND COMPARISON WITH *EX SITU* MEASUREMENTS

The method of ablative imprints applied to the focus size characterization goes back to early eighties of last century when Liu used first the contours imprinted by an optical laser beam on silicon crystals to estimate the transverse beam size in case of Gaussian beam.[10] The technique can be applied to the pulsed beams and has been noticed being particularly useful in case of strongly focused beam spots. The idea of the technique is fairly simple and based on tracing the beam profile by varying the beam intensity: since the contour of ablative imprints corresponds to the damage threshold, variation of overall beam intensity highlights cross-sections of different slices of the beam profile. The method has been recently demonstrated by working at VUV/XUV FEL for both Gaussian[7] and non-Gaussian[8] beam using PMMA as media for ablation, and extendable to shorter wavelengths in case of X-ray FEL with other suitably chosen materials to be ablated.[11]

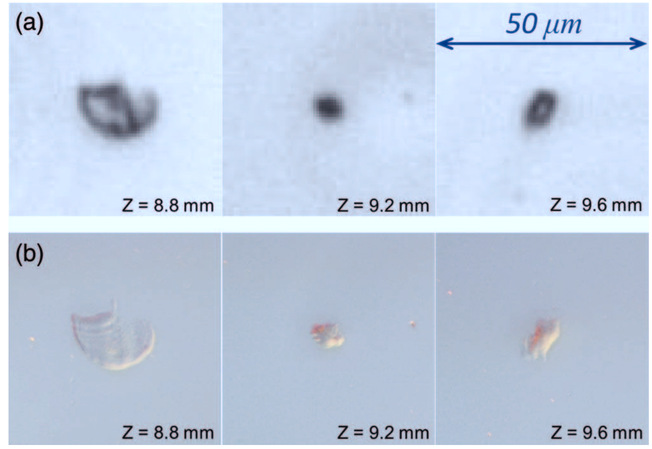

FIG. 3. Inspection of the imprints *in situ* by diagnostics port (a) and *ex situ* by Nomarski microscope (b).

To examine capabilities and limitations of the *in situ* beam profile characterization by using diagnostics port and ablative imprints technique, a comparison between *in situ* and *ex situ* measurements was done. For the sake of comparison, the imprints taken at FLASH earlier (in 2009) during an experiment with a super-polished off-axis parabolic mirror[12,13] were re-used. Goal of this former experiment was to achieve a sub-micrometer focus at wavelength of 13.5 nm. Micron-sized ablative imprints were inspected by both the diagnostics port (*in situ*) and Nomarski (DIC–differential interference contrast) microscope (*ex situ*). There are two advantages of such a virtual experiment. First, the imprints had already been thoroughly investigated by different techniques *ex situ* to retrieve accurate focus characterization. Second, small dimensions of the focused spot size and of corresponding ablative imprints, which are just beyond the capabilities of the diagnostics port, allow to determine the limitations.

A few images taken *in situ* by the diagnostics port and *ex situ* by Nomarski (DIC) microscope are presented in Fig. 3. They show both a good visibility of *in situ* inspection of ablative imprints contours on optically transparent PMMA samples and good representation of the contours shape. The latter is important for *in situ* optics alignment since it directly reflects aberrations to be corrected.

The imprints areas, enclosed by ablative threshold contour, were measured *in situ* and *ex situ*. The obtained results were compared, and this comparison is represented in Fig. 4(a) by a correlation plot. Linearity of the correlation plot evidences a good agreement between *in situ* and *ex situ* measurements, albeit the correlation slope does not exactly equal unity. Slightly higher slope value of (1.13 ± 0.01) is related to experimentalist's subjective error in ablation threshold contour identification. This immediately follows from lower

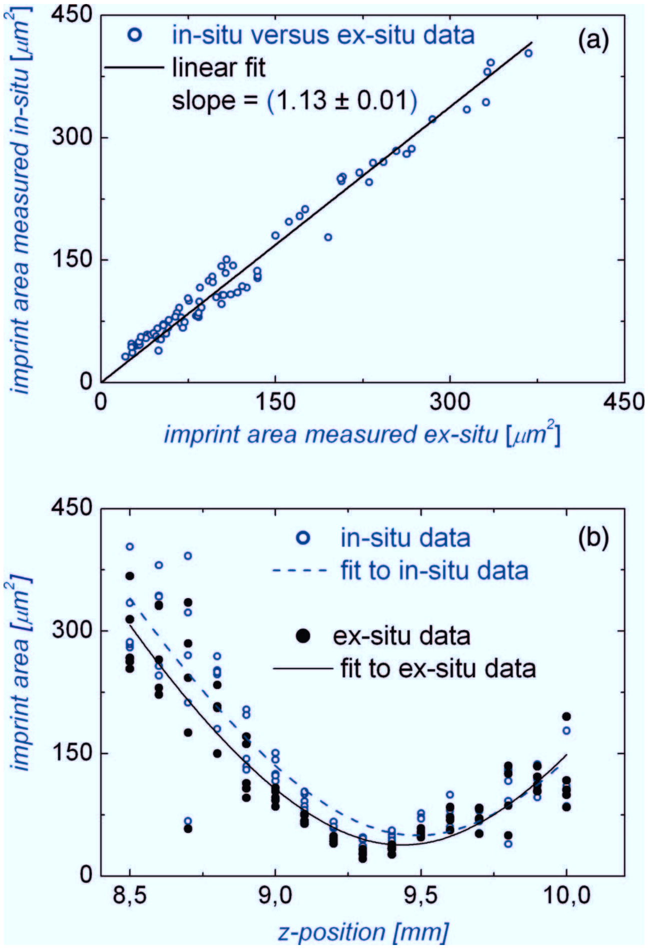

FIG. 4. Correlation plot of crater size estimation by *in situ* measurements using the diagnostics port versus Nomarski microscope (a) and caustic curves (b).

resolution of *in situ* images blurring otherwise sharp edges of ablation imprints (see Fig. 3 for comparison).

In order to gain a deeper insight into beam propagation properties, a z-scan (caustic scan) method[11] is usually exploited. For several longitudinal z-positions in close vicinity of the focus (beam waist) a few ablative imprints are recorded. The results of such measurements retrieved from both *in situ* and *ex situ* inspection are presented in Fig. 4(b). Model of a stigmatic Gaussian beam[11] was applied to measured ablation imprints areas plotted as a function of longitudinal z-position in order to enumerate the focal spot area, waist position, and Rayleigh range. The results are summarized in Table I. A good agreement between the main propagation parameters such as waist position and Rayleigh range was achieved. The focal spot area obtained by means of *in situ* measurements is slightly overestimated with respect to *ex situ* value due to the subjective error discussed above. Moreover, it should be noted that, in this particular case, both focal spot areas are overestimated owing to highly non-Gaussian nature of the beam for which the stigmatic Gaussian model usually fails. Typically, the results (except for the waist position) may depend on average attenuation level at which the z-scan is performed. This follows from the fact that different parts of the non-Gaussian beam (e.g., vicinity of the maximum, beam tails) may resemble a Gaussian beam of different parameters. Yet, the goal of this measurement was to compare the performance of the diagnostics port and Nomarski (DIC) microscope which is not affected by validity or invalidity of the model used.

TABLE I. Results of caustic curves parameters measured *in situ* (diagnostics port) and *ex situ* (Nomarski microscope).

The caustic property	*In situ* (diagnostics port)	*Ex situ* (Nomarski microscope)
Focal spot area (μm^2)	7.2 ± 2.5	4.7 ± 2.2
Waist position (mm)	9.49 ± 0.02	9.44 ± 0.02
Rayleigh range (mm)	0.32 ± 0.07	0.29 ± 0.07
Average peak-to-threshold ratio $\langle \ln(E/E_{th}) \rangle$	6.9 ± 2.8	8.2 ± 4.5

To conclude this section, it should be pointed out that *in situ* diagnostics tool provides excellent insight into performance of focusing optics used. Apparently, the optical resolution of the Navitar objective is much lower than of Nomarski microscope, which is primarily dictated by technically available working distance and numerical aperture (WD = 0.2 mm, NA = 1.3 for Nomarski 100× zoom objective; WD ≥ 78 mm, NA ≤ 0.1 for Navitar objective at maximum 7× zoom in presented set-up). However, the possibility of real-time inspection, being otherwise hardly feasible with Nomarski 100× zoom lens, represents a considerable benefit of long working distance microscopy despite the fact that the resolution is lower. Finally, we should highlight that a combination of the z-scan method and *in situ* measurements directly reveals fundamental aberrations of the focusing optics (e.g., astigmatism and coma) as stated above.

IV. COMPARISON BETWEEN ABLATIVE IMPRINTS AND FLUORESCENCE IMAGING

A qualitative comparison between the ablative imprint technique and imaging of the spot into visible fluorescence is presented in Fig. 5. The measurements were performed at FLASH running at 19 nm wavelength (65 eV photon energy) after the monochromator beamline PG2[14,15] operating in zeroth diffraction order. The imprints were taken on the

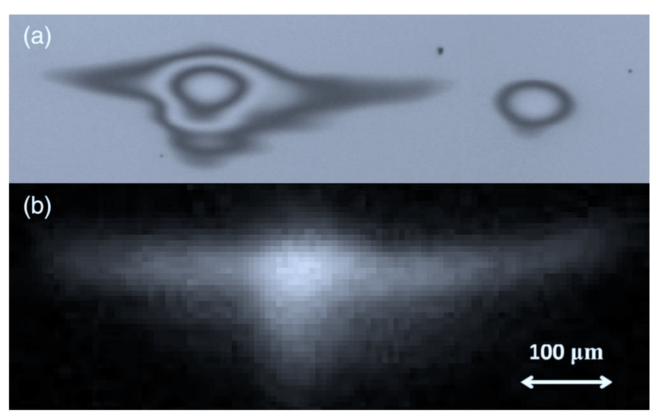

FIG. 5. The beam profile taken by ablative imprints (a) and with imaging crystal (b).

spin-coated with 0.5 μm PMMA samples, and the pulse energy on sample was varied from 2.5 μJ to 13 μJ. In Fig. 5(a) the left imprint corresponds to 12.9 μJ and the right to 2.8 μJ pulse energy. The resulting beam size in a Gaussian beam approximation was estimated to be (108 $\pm$ 17) μm FWHM in vertical and (149 $\pm$ 29) μm FWHM in horizontal direction. The imaging with YAG:Ce crystal was done at strong attenuation (down to 12 nJ) to avoid saturation effects leading to overestimation of the beam size. The resulted beam size (FWHM) for this particular shot is 89 μm in vertical direction and 152 μm in horizontal which is in good agreement with the ablation measurements.

As it has been mentioned above, the imaging of the XUV (highly) focused beams into optical fluorescence is limited by relatively low visible photon flux. The number of fluorescence photons could not be increased either by increasing volume of interaction of XUV photons with imaging crystal because of limited penetration depth (for instance, the penetration depth for 65 eV photons is 42 nm), or by increasing number of XUV photons because of saturation and quenching of the fluorescence. On the contrary, strong attenuation should be applied to avoid over-estimation of the beam size due to saturation: 3 orders of magnitude has been attenuated in the case presented here for the beam size above 100 μm, and even stronger by 3-4 order attenuation is needed when spot size reduces to few micrometers. The investigation of saturation effects is strongly wavelength dependent and should be done for each particular case. Yet, the number of photons could be increased in the case of multibunch operation acquiring light from up to hundreds of bunches. Summing visible light from pulse train on CCD is not affected by saturation since the separation between bunches in train is above 1 μs at FLASH, and this is slower than characteristic decay time of Ce luminescence in YAG. However, the pointing instabilities of SASE-based lasing could result in over-estimation of the beam size and smear out the spot shape in case of integrated multibunch acquisition.

Summarizing this section, for the beams focused down to 20 μm, both imaging crystal and ablative imprints methods implemented in our set-up could be used. A good agreement between the two methods achieved in this case confirms the reliability of the measurements. For the smaller beams, the ablative imprints provide fast and reliable diagnostics.

Finally, the diagnostics port has been successfully used at FLASH for the re-alignment of the focusing optics of the PG2 beamline. After the realignment, the FWHM spot size in focus has been reduced from above 100 μm to below 50 μm.

V. CONCLUSIONS

In conclusion, a portable low-cost tool has been built up allowing *in situ* focus characterization and enabling fast optics alignment at an XUV free electron laser source. The method of ablative imprints has been demonstrated being used *in situ* maintaining ultrahigh vacuum conditions needed to operate the XUV optics. The high contrast of inspection on transparent samples is reached using coaxial illumination. A good representation of the crates contours shape has been confirmed by comparison with *ex situ* analysis by Nomarski microscope. In this comparison, the focus sizes down to 3 μm have been demonstrated to be possible to characterized *in situ*.

ACKNOWLEDGMENTS

The authors are grateful to V. Rybnikov for assistance with dedicated software and to R. Sobierajski for useful discussion. The Czech co-authors appreciate funding by Grant Nos. LG13029, CZ.1.05/1.1.00/02.0061, CZ.1.07/2.3.00/20.0087, CZ.1.07/2.3.00/30.0057, 13-28721S, P108/11/1312, P205/11/0571, P208/10/2302, and M100101221.

[1] W. Ackermann, G. Asova, V. Ayvazyan, A. Azima, N. Baboi, J. Baehr, V. Balandin, B. Beutner, A. Brandt, A. Bolzmann, R. Brinkmann, O. I. Brovko, M. Castellano, P. Castro, L. Catani, E. Chiadroni, S. Choroba, A. Cianchi, J. T. Costello, D. Cubaynes, J. Dardis, W. Decking, H. Delsim-Hashemi, A. Delserieys, G. Di Pirro, M. Dohlus, S. Duesterer, A. Eckhardt, H. T. Edwards, B. Faatz, J. Feldhaus, K. Floettmann, J. Frisch, L. Froehlich, T. Garvey, U. Gensch, C. Gerth, M. Goerler, N. Golubeva, H.-J. Grabosch, M. Grecki, O. Grimm, K. Hacker, U. Hahn, J. H. Han, K. Honkavaara, T. Hott, M. Huening, Y. Ivanisenko, E. Jaeschke, W. Jalmuzna, T. Jezynski, R. Kammering, V. Katalev, K. Kavanagh, E. T. Kennedy, S. Khodyachykh, K. Klose, V. Kocharyan, M. Koerfer, M. Kollewe, W. Koprek, S. Korepanov, D. Kostin, M. Krassilnikov, G. Kube, M. Kuhlmann, C. L. S. Lewis, L. Lilje, T. Limberg, D. Lipka, F. Loehl, H. Luna, M. Luong, M. Martins, M. Meyer, P. Michelato, V. Miltchev, W. D. Moeller, L. Monaco, W. F. O. Mueller, O. Napieralski, O. Napoly, P. Nicolosi, D. Noelle, T. Nunez, A. Oppelt, C. Pagani, R. Paparella, N. Pchalek, J. Pedregosa-Gutierrez, B. Petersen, B. Petrosyan, G. Petrosyan, L. Petrosyan, J. Pflueger, E. Ploenjes, L. Poletto, K. Pozniak, E. Prat, D. Proch, P. Pucyk, P. Radcliffe, H. Redlin, K. Rehlich, M. Richter, M. Roehrs, J. Roensch, R. Romaniuk, M. Ross, J. Rossbach, V. Rybnikov, M. Sachwitz, E. L. Saldin, W. Sandner, H. Schlarb, B. Schmidt, M. Schmitz, P. Schmueser, J. R. Schneider, E. A. Schneidmiller, S. Schnepp, S. Schreiber, M. Seidel, D. Sertore, A. V. Shabunov, C. Simon, S. Simrock, E. Sombrowski, A. A. Sorokin, P. Spanknebel, R. Spesyvtsev, L. Staykov, B. Steffen, F. Stephan, F. Stulle, H. Thom, K. Tiedtke, M. Tischer, S. Toleikis, R. Treusch, D. Trines, I. Tsakov, E. Vogel, T. Weiland, H. Weise, M. Wellhoeffer, M. Wendt, I. Will, A. Winter, K. Wittenburg, W. Wurth, P. Yeates, M. V. Yurkov, I. Zagorodnov, and K. Zapfe, Nature Photon. **1**, 336 (2007).

[2] P. Emma, R. Akre, J. Arthur, R. Bionta, C. Bostedt, J. Bozek, A. Brachmann, P. Bucksbaum, R. Coffee, F. J. Decker, Y. Ding, D. Dowell, S. Edstrom, A. Fisher, J. Frisch, S. Gilevich, J. Hastings, G. Hays, P. Hering, Z. Huang, R. Iverson, H. Loos, M. Messerschmidt, A. Miahnahri, S. Moeller, H. D. Nuhn, G. Pile, D. Ratner, J. Rzepiela, D. Schultz, T. Smith, P. Stefan, H. Tompkins, J. Turner, J. Welch, W. White, J. Wu, G. Yocky, and J. Galayda, Nature Photon. **4**, 641 (2010).

[3] I. Ishikawa, H. Aoyagi, T. Asaka, Y. Asano, N. Azumi, T. Bizen, H. Ego, K. Fukami, T. Fukui, Y. Furukawa, S. Goto, H. Hanaki, T. Hara, T. Hasegawa, T. Hatsui, A. Higashiya, T. Hirono, N. Hosoda, M. Ishii, T. Inagaki, Y. Inubushi, T. Itoga, Y. Joti, M. Kago, T. Kameshima, H. Kimura, Y. Kirihara, A. Kiyomichi, T. Kobayashi, C. Kondo, T. Kudo, H. Maesaka, X. M. Marechal, T. Masuda, S. Matsubara, T. Matsumoto, T. Matsushita, S. Matsui, M. Nagasono, N. Nariyama, H. Ohashi, T. Ohata, T. Ohshima, S. Ono, Y. Otake, C. Saji, T. Sakurai, T. Sato, K. Sawada, T. Seike, K. Shirasawa, T. Sugimoto, S. Suzuki, S. Takahashi, H. Takebe, K. Takeshita, K. Tamasaku, H. Tanaka, R. Tanaka, T. Tanaka, T. Togashi, K. Togawa, A. Tokuhisa, H. Tomizawa, K. Tono, S. Wu, M. Yabashi, M. Yamaga, A. Yamashita, K. Yanagida, C. Zhang, T. Shintake, H. Kitamura, and N. Kumagai, Nature Photon. **6**, 540 (2012).

[4] H. Yumoto, H. Mimura, T. Koyama, S. Matsuyama, K. Tono, T. Togashi, Y. Inubushi, T. Sato, T. Tanaka, T. Kimura, H. Yokoyama, J. Kim, Y. Sano, Y. Hachisu, M. Yabashi, H. Ohashi, H. Ohmori, T. Ishikawa and K. Yamauchi, Nature Photon. **7**, 43 (2012).

[5] P. Mercère, P. Zeitoun, M. Idir, S. L. Pape, D. Douillet, X. Levecq, G. Dovillaire, S. Bucourt, K. A. Goldberg, P. P. Naulleau, and S. Rekawa, Opt. Lett. **28**, 1534 (2003).

[6] B. Flöter, P. Juranic, S. Kapitzki, B. Keitel, K. Mann, E. Plönjes, B. Schäfer, and K. Tiedtke, New J. Phys. **12**, 083015 (2010).

[7] J. Chalupský, L. Juha, J. Kuba, J. Cihelka, V. Hájková, S. Koptyaev, J. Krása, A. Velyhan, M. Bergh, C. Caleman, J. Hajdu, R. M. Bionta, H. Chapman, S. P. Hau-Riege, R. A. London, M. Jurek, J. Krzywinski, R. Nietubyc, J. B. Pelka, R. Sobierajski, J. Meyer-Ter-Vehn, A. Tronnier, K. Sokolowski-Tinten, N. Stojanovic, K. Tiedtke, S. Toleikis, T. Tschentscher, H. Wabnitz, and U. Zastrau, Opt. Express **15**, 6036 (2007).
[8] J. Chalupský, J. Krzywinski, L. Juha, V. Hájková, J. Cihelka, T. Burian, L. Vyšín, J. Gaudin, A. Gleeson, M. Jurek, A. R. Khorsand, D. Klinger, H. Wabnitz, R. Sobierajski, M. Störmer, K. Tiedtke, and S. Toleikis, Opt. Express **18**, 27836 (2010).
[9] A. Singer, F. Sorgenfrei, A. P. Mancuso, N. Gerasimova, O. M. Yefanov, J. Gulden, T. Gorniak, T. Senkbeil, A. Sakdinawat, Y. Liu, D. Attwood, S. Dziarzhytski, D. D. Mai, R. Treusch, E. Weckert, T. Salditt, A. Rosenhahn, W. Wurth, and I. A. Vartanyants, Opt. Express **20**, 17480 (2012).
[10] J. M. Liu, Opt. Lett. **7**, 196 (1982).
[11] J. Chalupsky, P. Bohacek, V. Hajkova, S. P. Hau-Riege, P. A. Heimann, L. Juha, J. Krzywinski, M. Messerschmidt, S. P. Moeller, B. Nagler, M. Rowen, W. F. Schlotter, M. L. Swiggers, and J. J. Turner, Nucl. Instrum. Methods Phys. Res. A **631**, 130 (2011).
[12] S. Bajt, H. N. Chapman, A. J. Nelson, R. W. Lee, S. Toleikis, P. Mirkarimi, J. B. Alameda, S. L. Baker, H. Vollmer, R. T. Graff, A. Aquila, E. M. Gullikson, J. Meyer Ilse, E. A. Spiller, J. Krzywinski, L. Juha, J. Chalupský, V. Hájková, J. Hajdu, and T. Tschentscher, Proc. SPIE **7361**, 73610J (2009).
[13] A. J. Nelson, S. Toleikis, H. Chapman, S. Bajt, J. Krzywinski, J. Chalupsky, L. Juha, J. Cihelka, V. Hajkova, L. Vysin, T. Burian, M. Kozlova, R. R. Fäustlin, B. Nagler, S. M. Vinko, T. Whitcher, T. Dzelzainis, O. Renner, K. Saksl, A. R. Khorsand, P. A. Heimann, R. Sobierajski, D. Klinger, M. Jurek, J. Pelka, B. Iwan, J. Andreasson, N. Timneanu, M. Fajardo, J. S. Wark, D. Riley, T. Tschentscher, J. Hajdu, and R. W. Lee, Opt. Express **17**, 18271 (2009).
[14] M. Martins, M. Wellhoefer, J. T. Hoeft, W. Wurth, J. Feldhaus, and R. Follath, Rev. Sci. Instrum. **77**, 115108 (2006).
[15] N. Gerasimova, S. Dziarzhytski, and J. Feldhaus, J. Mod. Opt. **58**, 1480 (2011).